

Supporting Information

Du and Zatorre 10.1073/pnas.1712223114

SI Text

Multivoxel Pattern Analysis. First, univariate trialwise β coefficients for all brain voxels were estimated from the concatenated data using AFNI program 3dLSS (Least Square Sum regression; ref. 1). Then Freesurfer's automatic anatomical parcellation (aparc2009; ref. 2) algorithm was used to define a set of 152 cortical and subcortical ROIs from individual's high-resolution anatomical scan. Next, ROIs known to be sensitive to speech production and perception were selected. This was done by first creating a meta-analytic mask on Neurosynth (3) using the search term "speech." It resulted in a coordinate-based activation mask constructed from 424 studies and encompassing the language-related areas in the temporal and frontal lobes. This metaanalytic mask was then intersected with the Freesurfer ROI mask defined in MNI space. If any of the intersected ROIs had more than 10 voxels, they were included in further analyses. To ensure hemispheric symmetry, if a left hemisphere ROI was included, so was its right hemisphere homolog. This eventually resulted in 42 ROIs (21 left and 21 right; Fig. 2J) that were used in MVPA.

MVPA were then carried out in the volumetric space within anatomical ROIs at each noise level, using shrinkage discriminant analysis (4) as implemented in the R package sda. Shrinkage discriminant analysis is a form of linear discriminant analysis that estimates shrinkage parameters for the variance-covariance

matrix of the data, making it suitable for high-dimensional classification problems. To evaluate classifier performance, fivefold cross-validation where each fold of data consisted of the β regression weights of four out of five runs was used, with one run held out for testing. The shrinkage discriminant classifier produces both a categorical prediction (i.e., the label of the test case) as well as a continuous probabilistic output (the posterior probability that the test case is of label x). The continuous outputs were used to compute the AUC metrics, and the AUC scores were used as an index of classification performance because they are robust to class imbalances and are better able to incorporate the relationship between probabilistic classifier output and discrete category membership. As the experiment had four phoneme categories, a multiclass AUC measure that was computed as the average of all of the pairwise two-class AUC scores was used.

Because MVPA was conducted in anatomically defined ROIs specific to each participant, no spatial normalization was applied. Notably, although the classification may capture the button/finger decoding in addition to the phoneme category decoding in the left dorsal preCG (hand area), any response-related activity should not be affected by noise level or musical experience, which are the focus of this study.

1. Mumford JA, Turner BO, Ashby FG, Poldrack RA (2012) Deconvolving BOLD activation in event-related designs for multivoxel pattern classification analyses. *Neuroimage* 59: 2636–2643.
2. Destrieux C, Fischl B, Dale A, Halgren E (2010) Automatic parcellation of human cortical gyri and sulci using standard anatomical nomenclature. *Neuroimage* 53:1–15.

3. Yarkoni T, Poldrack RA, Nichols TE, Van Essen DC, Wager TD (2011) Large-scale automated synthesis of human functional neuroimaging data. *Nat Methods* 8: 665–670.
4. Ahdesmäki M, Strimmer K (2010) Feature selection in omics prediction problems using cat scores and false non-discovery rate control. *Ann Appl Stat* 4:503–519.

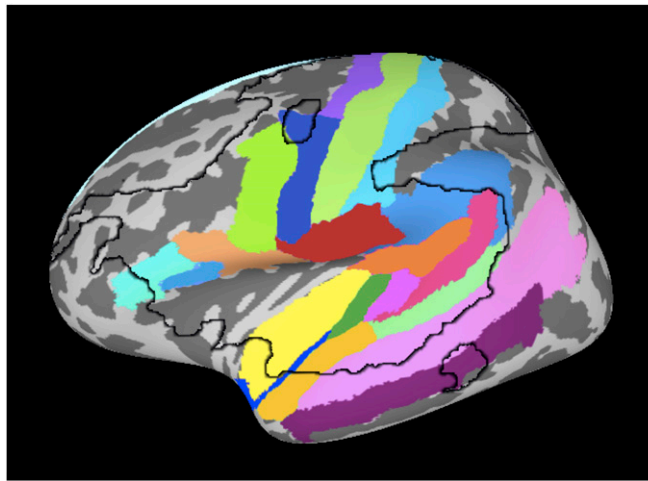


Fig. S1. Speech-related ROIs used in MVPA were activated by the syllable in noise identification task in our participants. Speech-related ROIs were selected by intersecting a Neurosynth automated metaanalysis (search term: speech) and 152 Freesurfer anatomical ROIs (aparc 2009 atlas). The black contour outlines the BOLD activation elicited by syllable identification across all of the conditions and participants ($P_{FWE} < 0.001$). Note that the BOLD contour nicely overlapped with the distribution of ROIs.

Table S1. Details of musicians' musical experience

Participant ID	Years of training	Age of onset, y	Type of training
1	18	5	Piano, flute, guitar
2	12	7	Bass, guitar, voice
3	12	7	Piano, flute, voice
4	12	7	Piano, voice, saxophone
5	15	4	Piano, guitar, drum, voice
6	14	7	Voice
7	11	7	Bass, piano
8	22	3	Oboe, piano
9	16	5	Piano, harpsichord
10	17	6	Clarinet
11	18	5	Piano, flute, bassoon
12	24	4	Piano, flute, voice
13	19	3	Piano, trumpet, flute, voice
14	18	3	Piano, voice, clarinet, trumpet
15	16	4	Piano, trumpet

Table S2. Descriptive statistics and t tests for demographics and cognitive tasks

Item	Musicians ($n = 15$), Mean (SD)	Nonmusicians ($N = 15$), Mean (SD)	t value (P value)
Age, y	21.4 (2.7)	22.1 (4.4)	-0.55 (0.59)
Postsecondary education, y	2.5 (1.7)	2.5 (1.5)	0.11 (0.91)
Pure-tone average, dB HL	4.5 (2.2)	4.6 (2.5)	-0.11 (0.91)
Digit span	12.1 (2.2)	11.9 (2.2)	0.25 (0.81)
Culture fair intelligence	30.1 (4.7)	29.3 (4.2)	0.51 (0.62)

Table S3. Regions showing significantly higher activity in musicians than nonmusicians ($P_{FWE} < 0.001$)

Regions	BA	Peak Talairach coordinate			T value	No. of voxels
		x	y	z		
R inferior parietal lobule	40	38	-52	44	4.74	32
R superior/middle temporal gyrus	22, 21	47	-28	-1	4.53	12
L inferior frontal gyrus	45	-51	22	15	4.10	4

Table S4. Regions with significant (false discovery rate corrected $P < 0.05$) phoneme classification at each SNR in each group

SNR	Region of interest	AUC score	t	Uncorrected p	Cohen's d		
Musician							
No noise	L inferior insula	0.527	3.235	0.006	0.835		
	L Heschl's gyrus	0.533	3.388	0.004	0.875		
	L posterior superior temporal gyrus	0.539	3.297	0.005	0.851		
	L superior temporal sulcus	0.524	3.229	0.006	0.834		
	L middle temporal gyrus	0.523	2.817	0.014	0.727		
	L planum temporale	0.528	2.724	0.016	0.933		
	L supramarginal gyrus	0.539	3.782	0.002	0.976		
	L postcentral gyrus	0.594	8.333	0.000	2.152		
	L central sulcus	0.552	4.866	0.000	1.257		
	L ventral precentral gyrus	0.550	5.784	0.000	1.493		
	L dorsal precentral gyrus	0.554	7.415	0.000	1.915		
	L inferior frontal - pars opercularis	0.547	4.006	0.001	1.096		
	L inferior frontal - pars triangularis	0.533	4.557	0.000	1.177		
	R inferior insula	0.535	2.909	0.011	0.751		
	R Heschl's gyrus	0.533	3.420	0.004	0.883		
	R posterior superior temporal gyrus	0.529	4.188	0.001	1.081		
	R planum temporale	0.532	2.828	0.013	0.730		
	R postcentral gyrus	0.548	5.007	0.000	1.293		
	R ventral precentral gyrus	0.534	3.611	0.003	0.932		
	R dorsal precentral gyrus	0.537	3.094	0.008	0.799		
	R inferior frontal - pars opercularis	0.535	2.725	0.016	0.704		
	8 dB	L Heschl's gyrus	0.535	2.901	0.012	0.749	
		L posterior superior temporal gyrus	0.532	3.248	0.006	0.839	
		L superior temporal sulcus	0.530	2.790	0.014	0.720	
		L planum temporale	0.531	3.170	0.007	0.818	
		L posterior lateral fissure	0.536	3.005	0.009	0.776	
		L supramarginal gyrus	0.536	4.424	0.001	1.164	
		L subcentral gyrus/sulcus	0.538	3.014	0.009	0.778	
L postcentral gyrus		0.597	5.600	0.000	1.446		
L central sulcus		0.556	3.030	0.009	0.782		
L ventral precentral gyrus		0.551	3.856	0.002	0.996		
L dorsal precentral gyrus		0.580	8.023	0.000	2.071		
L inferior frontal - pars opercularis		0.546	4.306	0.001	1.105		
R posterior superior temporal gyrus		0.538	3.113	0.008	0.804		
R postcentral gyrus		0.541	2.900	0.012	0.749		
R ventral precentral gyrus		0.533	3.393	0.004	0.876		
R dorsal precentral gyrus		0.538	3.262	0.006	0.842		
0 dB		L posterior superior temporal gyrus	0.528	3.617	0.003	0.934	
		L planum temporale	0.531	3.101	0.008	0.853	
		L postcentral gyrus	0.597	5.904	0.000	1.524	
		L central sulcus	0.536	3.326	0.005	0.859	
		L ventral precentral gyrus	0.540	3.072	0.008	0.793	
		L dorsal precentral gyrus	0.571	4.286	0.001	1.107	
		L inferior frontal - pars opercularis	0.539	3.283	0.005	0.906	
		R posterior superior temporal gyrus	0.539	3.283	0.005	0.848	
		-4 dB	L posterior superior temporal gyrus	0.538	3.399	0.004	0.878
			L planum temporale	0.530	3.656	0.003	1.120
			L postcentral gyrus	0.585	6.063	0.000	1.565
			L central sulcus	0.553	5.262	0.000	1.359
L ventral precentral gyrus	0.537		3.671	0.003	0.948		
L dorsal precentral gyrus	0.563		4.738	0.000	1.223		
-8 dB	L inferior frontal - pars opercularis	0.536	3.696	0.002	0.954		
	L postcentral gyrus	0.564	4.604	0.000	1.189		
	L ventral precentral gyrus	0.529	4.363	0.001	1.126		
Nonmusician	L dorsal precentral gyrus	0.540	3.713	0.002	0.959		
	No noise						
	L posterior superior temporal gyrus	0.536	3.131	0.007	0.808		
	L planum temporale	0.526	3.159	0.007	0.816		
	L supramarginal gyrus	0.525	3.300	0.005	0.852		
	L postcentral gyrus	0.571	4.163	0.001	1.075		
	L ventral precentral gyrus	0.533	4.126	0.001	1.065		

Table S4. Cont.

SNR	Region of interest	AUC score	<i>t</i>	Uncorrected <i>p</i>	Cohen's <i>d</i>
8 dB	L dorsal precentral gyrus	0.557	4.227	0.001	1.091
	L inferior frontal - pars opercularis	0.535	3.885	0.002	1.386
	L inferior frontal - pars triangularis	0.526	3.175	0.007	0.820
	R posterior superior temporal gyrus	0.529	3.016	0.009	0.779
	R postcentral gyrus	0.535	2.933	0.011	0.757
	L postcentral gyrus	0.569	4.046	0.001	1.045
	L ventral precentral gyrus	0.537	3.255	0.006	0.840
	L dorsal precentral gyrus	0.538	3.607	0.003	0.946
	L inferior precentral sulcus	0.547	4.212	0.001	1.088
	L inferior frontal – pars opercularis	0.535	3.311	0.005	1.193
0 dB	L inferior frontal – pars triangularis	0.052	4.271	0.001	1.103
	L postcentral gyrus	0.563	3.448	0.004	0.890
	L central sulcus	0.536	4.077	0.001	1.053
	L ventral precentral gyrus	0.536	3.213	0.006	0.830
	L dorsal precentral gyrus	0.558	4.842	0.000	1.250
–4 dB	L inferior frontal – pars opercularis	0.530	3.691	0.002	0.953
	L postcentral gyrus	0.569	4.045	0.001	1.044

Table S5. Regions showing significant psychophysiological interactions with the auditory seed ($P_{FWE} < 0.01$)

Regions	BA	Peak Talairach coordinate			<i>t/F</i> value	No. of voxels
		<i>x</i>	<i>y</i>	<i>z</i>		
Left auditory seed						
Musician > nonmusician						
R inferior frontal gyrus	45, 44	50	19	16	3.33	18
L dorsal premotor cortex	6	–36	–7	42	3.33	8
Nonmusician > musician						
R cerebellum	NA	8	–76	–22	–3.86	14
Right auditory seed						
Musician > nonmusician						
R inferior frontal gyrus	44, 45	50	16	18	3.42	78
L primary motor cortex	4	–34	–16	50	3.79	30
R Heschl's gyrus	42	56	–13	11	3.25	10
Nonmusician > musician						
R cerebellum	NA	8	–70	–31	–3.70	14
Group × SNR						
R anterior superior temporal gyrus	38	53	11	–13	4.50	10
L angular gyrus	39	–43	–58	30	3.70	8
L ventral premotor cortex	6, 9	–50	4	32	4.03	8
R ventral premotor cortex	6	56	–1	32	4.00	6

The *t* values were presented for the contrast of musician > nonmusician, whereas the *F* values were presented for the group by SNR interaction.